JOURNAL OF MATERIALS SCIENCE 25 (1990) 5207–5214

Mn and Co substitution in δ-FeOOH and its decomposition products

J. M. JIMÉNEZ MATEOS, M. MACÍAS*, J. MORALES, J. L. TIRADO
Departamento de Química Inorgánica e Ingeniería Química, Facultad de Ciencias, Universidad de Córdoba, 14004 Córdoba, Spain

Cobalt and manganese substituted δ-FeOOH were obtained and used in the preparation of Fe, Co and Mn, Fe mixed oxides. Cobalt is present in the oxyhydroxide with 2.8–3.0, oxidation states. Lattice parameters and oxidation state decrease with cobalt content. Mn-substituted phases contain manganese in oxidation states decreasing from 4.0 to 3.3 as the degree of substitution is higher. These Mn-oxidation states imply cation vacancies which are alternatively ordered in octahedral sites along the [0 0 1] direction of the δ-oxyhydroxide structure. The thermal decomposition of the cobalt and Mn-substituted samples at 200° C leads to mixed oxides with distorted α-Fe_2O_3 structure and high manganese and cobalt oxidation states. From 200 to 400° C, a reduction process takes place, leading to Mn-substituted sesquioxides, while Co-containing samples decompose into mixtures of spinel and α-Fe_2O_3-structure phases.

1. Introduction

The use of a precursor compounds of transition metal oxides is a straightforward route in the preparation of metastable modications by thermal decomposition reactions [1]. In this way, it has been found that the low-temperature decomposition of carbonate precursors containing manganese leads to oxides with high metal oxidation states [2, 3]. For these purposes, the use of complex hydroxides is limited by their gelatinous characteristics that contain variable quantities of adsorbed ions that are not easily washed thoroughly. In contrast, some cation-substituted oxyhydroxide phases can be prepared as high purity compounds and may be used as alternative precursors.

Substitution by divalent and trivalent metal ions in δ-FeOOH was described by Petit [4] and Okamoto [5]. More recently, Muller *et al.* [6–8] studied divalent metal (Zn, Mg, Cd and Ca) substitution in δ-FeOOH and showed that the solid solutions had compositions of the type $Fe_{1-x}M_xO_{1-x}(OH)_{1+x}$. Additionally, these authors found that the thermal decomposition of the δ-phases leads to α-Fe_2O_3-based solid solutions at low temperatures.

The occurrence of highly distorted modifications of α-Fe_2O_3 by the thermal and mechanochemical decomposition of pure δ-FeOOH was recently examined by X-ray diffraction line profile analysis [9, 10] and a high content of lattice distortions along the *c*-axis of the oxide was detected.

In this paper, δ-oxyhydroxide phases with partial substitution of iron by cobalt and manganese ions are prepared and studied as precursor compounds in the preparation of Fe, Co and Mn, Fe mixed oxides.

2. Experimental details

Manganese and cobalt substituted δ-FeOOH were prepared by careful oxidation of aqueous suspension of divalent metal hydroxides with 30% H_2O_2. The hydroxides were obtained from reagent grade $FeSO_4 \cdot 7H_2O$, $MnSO_4 \cdot H_2O$ and $Co(NO_3)_2 \cdot 6H_2O$ dissolved in distilled water ($[M^{2+}]_{total} = 0.3$ M), after oxygen elimination by argon bubbling. Under an argon atmosphere, 2 M NaOH was added with 3 : 2 volume ratio. The suspension was heated at 60° C for 5 to 10 min prior to the H_2O_2 addition (5 : 1 volume ratio). Then, the oxyhydroxide suspension was poured on cold water and floculated after 24 h. The precipitate was then washed with distilled water by decantation until peptization occurred, and dried at 60° C for 3 to 4 days, crushed to a fine powder and dried in a vacuum desiccator over P_4O_{10} for 5 to 7 days.

The degree of manganese and cobalt substitution was evaluated from the metal ratios determined by electron microprobe, X-ray ED microanalysis and atomic absorption spectrometry. The average oxidation state of metal ions in the samples was determined by the following procedure. About 150 mg of the oxyhydroxide samples and 50 mg of oxide samples were dissolved in 5 to 15 ml of 0.1 M Fe^{2+}, 10 ml of conc H_2SO_4 and 10 ml of H_2O, under a continuous flow of argon, and heated until complete dissolution. After cooling to 20 to 25° C, 10 ml of 85% H_3PO_4, 25 ml of H_2O and 0.15 ml of indicator (3% diphenilamine in ethanol) were added. The solution was titrated with standard 0.05 M K_2CrO_7. The difference between this titration and a blank titration was assigned to the total content of oxidizing species (Co(III), Mn(III)

* *Present address*: Departamento Química Inorgánica, Facultad de Química, Universidad de Sevilla, Spain.

0022–2461/90 $03.00 + .12

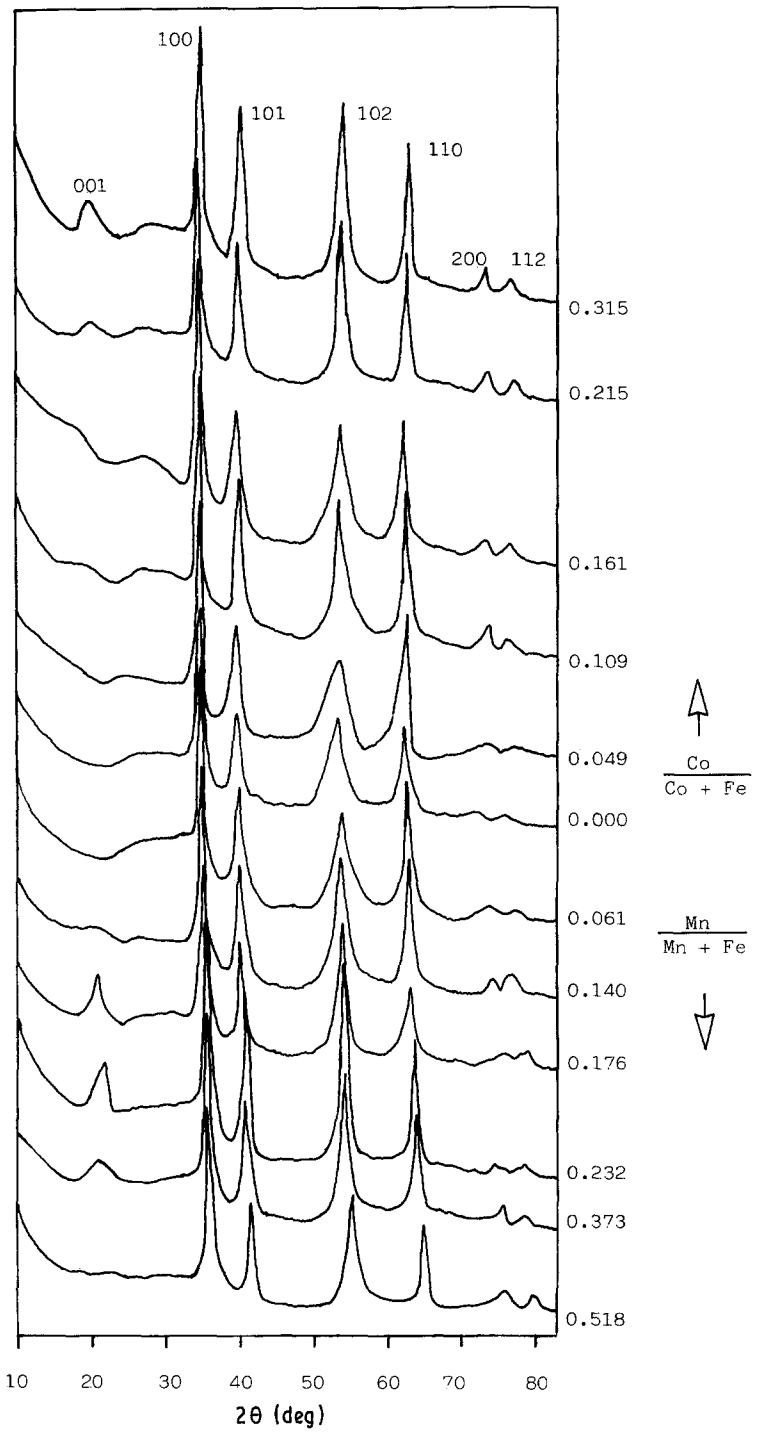

Figure 1 X-ray diffraction patterns of cobalt and manganese substituted δ-oxyhydroxide phases.

and Mn(IV)). On the other hand, Fe, Mn and Co contents in the samples were determined by atomic absorption spectrometry. From these data, the mean oxidation state of Co and Mn in Co-substituted and Mn-substituted δ-FeOOH were determined.

The X-ray diffraction patterns were obtained with a Siemens D501 diffractometer, provided with CuK_α radiation and graphite monochromator. The data collection by the step-scan technique (0.02° θ step width) and background correction were performed with a DACO-MP system. Silicon and Co_3O_4 were used as standards in the determination of lattice constants and line-broadening analysis. The analysis of the profiles was done by profile fitting to Pearson VII functions, according to the method described by de Keijser *et al.* [11]. For the overlapping 1 1 0 and 1 0 4 reflections of haematite, a separation procedure was developed by simultaneous fitting to P-VII functions.

Differential scanning calorimetry (DSC) traces were obtained with a Mettler TA3000 apparatus. Thermogravimetric (TG) traces were recorded with a Cahn 2000 electrobalance. Thermally decomposed samples were prepared by isothermal treatment of the oxyhydroxides at selected temperatures for 1 h. Electron micrographs were obtained with a JEOL 200CX microscope.

3. Results and discussion

The preparation procedure used in this study allows the synthesis of high-purity δ-oxyhydroxide phases in a wide interval of composition, as revealed by XRD (Fig. 1). The presence of a broad band between 20 and 35° 2θ which is also found in other studies of δ-oxyhydroxide [4, 12] should not be ascribed to the presence of amorphous components, as shown by electron microscopy (Fig. 2). The presence of surface

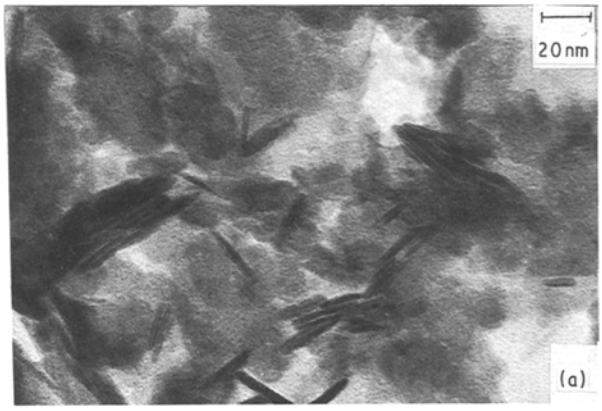

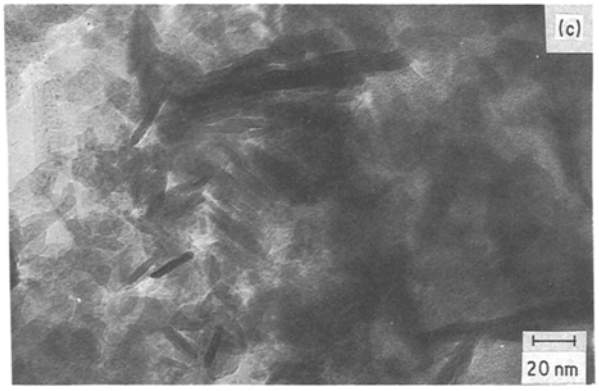

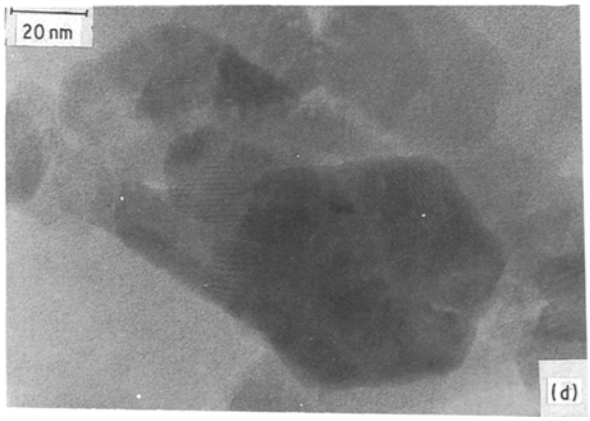

Figure 2 Electron micrographs (a) pure, (b) Co-containing (x_{Co} = 0.215) and (c) Mn-containing (x_{Mn} = 0.140) δ-oxhhydroxide. Samples prepared at 200° C: bright field (d) x_{Co} = 0.215 and (e) x_{Mn} = 0.232; dark-field (f) x_{Co} = 0.215 and (g) x_{Mn} = 0.232.

water may be responsible for this effect, as the intensity of the band decreases with desiccation treatment. The cation substitution limits were 30% for cobalt and 50% for manganese. Above these limits, the occurrence of significant amounts of spinel-structure and α-FeOOH phases was detected. The oxidation states of the substituent metals (Table I) are high. For Co-containing samples, the oxidation state of cobalt is always higher than 2.5 and decreases with cobalt content. These values imply the presence of significant amounts of Co(II) in the oxyhydroxide phases. In analogy with other divalent metal substituted derivatives [6], the electroneutrality may be maintained by compositions as $Fe^{III}_{1-x-y}Co^{III}_{y}Co^{II}_{x}O_{1-x}(OH)_{1+x}$. For Mn-containing samples, the oxidation states are higher than 3 in the complete composition interval and decrease with manganese content. The oxidation of Mn(II) by H_2O_2 in the preparation conditions is responsible for these high oxidation states. The presence of tetravalent ions in the structure of δ-oxyhydroxide may be explained by assuming a cation-deficient phase, as found in other structures as spinel phases [3].

On the other hand, the values of unit cell parameters of the oxyhydroxide samples are shown in Table I. A significant decrease of both a and c is observed in Co-substituted samples, in agreement with the composition and ionic radius of low-spin Co(III) ions. For Mn-containing samples, the sequence in the values of unit cell parameters can be considered as a consequence of the presence of variable contents of Mn(IV) and Mn(III) ions and the dependence of these contents with the level of substitution.

Additionally, a closer inspection of the XRD data in Fig. 1 reveals changes in the relative intensity of the 0 0 1 reflection of the δ phases, specially in Mn-substituted samples. These changes are in a direct relationship with the evolution of c and a. It is known that the intensity of this line is markedly affected by several factors [6, 13], as defects along the c direction that disrupt the crystalline periodicity or the cation distribution between the two octahedral sublattices of the structure (1a and 1b equivalent positions of the $P\bar{3}$ m1 space group). For Zn-substitution, the inclusion of zinc ions in the 1a sites exclusively was proven [6] to induce differences in the atomic scattering factors of both sublattices, thus increasing the 0 0 1 line intensity.

As the atomic scattering factors of Fe(III), Mn(III) or Mn(IV) are close, cation distribution in fully

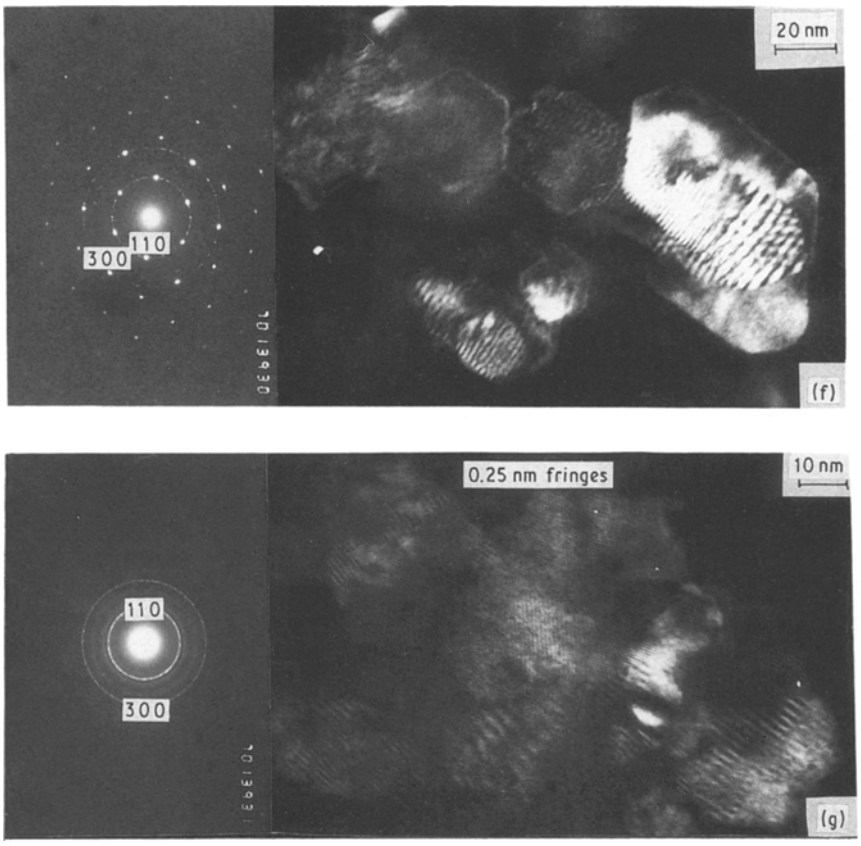

Figure 2 Continued

occupied 1a and 1b positions could not explain an enhanced intensity. In this way, XRD data on Mn(III)-substituted δ-FeOOH do not show the 0 0 1 reflection, as reported in [4]. Instead, if the presence of Mn(IV) implies cation vacancies, as suggested above, and these vacancies are preferentially placed in one of these sets of equivalent positions, the intensity of the 0 0 1 reflection may be considerably enhanced. Probably the presence of imperfections along the c axis may also be involved in the changes in intensity ratios observed in Fig. 1. For Co-substituted δ-FeOOH, the intensity of the 0 0 1 line is only observable for high cobalt contents. For these samples, the lower content in imperfections along the c axis, as discussed below, may be responsible for this behaviour. However, the possible ordering of (Co^{II}, Co^{III}) and (Fe^{III}) cations in both sublattices may also be implied in the low-intensity 0 0 1 line occurrence for high cobalt contents.

The electron micrographs of the oxyhydroxide samples (Fig. 2a to c) showed that cobalt or manganese substitution had little effect on particle size and shape. On the other hand, the integral breadth values in Table I show that the solid solutions do not increase markedly their crystallinity in all the crystallographic directions considered in the analysis, as compared with pure δ-FeOOH. This behaviour is different to that found in other crystalline modification of iron oxyhydroxide, as Mn-substituted α-FeOOH, where an increase in crystallite size was detected [14]. However, for Co-substituted phases, a decrease in β is observed for 10l lines. This effect has been interpreted in Zn-substituted oxyhydroxide [6] as a result of an increase in the thickness of the platelike particles. For Mn-containing phases, the effect is also complex. In this system there is no divalent-metal substitution. Instead, for those samples with Mn oxidation state closer to 4, crystallinity increases with Mn-content. For higher Mn-contents, Mn(III) is simultaneously included in the structure, and conditions a decrease in crystallinity.

TABLE I Stoichiometry and structural parameters of manganese and cobalt substituted δ-FeOOH

Parameters	Mn, Fe						Fe	Co, Fe				
x*	0.518	0.373	0.232	0.176	0.140	0.061	0.000	0.049	0.109	0.161	0.215	0.315
n†	3.334	3.518	3.771	4.000	4.000	4.000	–	2.836	2.759	2.731	2.665	2.591
a‡	0.2896	0.2899	0.2909	0.2917	0.2933	0.2939	0.2951	0.2947	0.2943	0.2942	0.2937	0.2927
c‡	0.4498	0.4481	0.4486	0.4496	0.4514	0.4525	0.4538	0.4520	0.4509	0.4506	0.4501	0.4493
β_1	0.796	1.235	1.171	1.367	1.143	–	1.044	–	0.946	1.021	1.096	1.064
β_2	1.592	1.560	1.089	1.237	1.540	–	1.730	–	1.334	1.205	1.240	1.252
β_3	2.334	1.983	1.418	1.458	2.049	–	2.626	–	2.130	1.655	1.621	1.783
β_4	1.420	1.392	1.079	1.369	1.086	–	1.166	–	0.926	1.141	1.149	1.082

*x = M/(M + Fe); M = Co, Mn.
†Oxidation state of M.
‡Unit cell parameters (± 0.0002 nm).
$\beta_{1,2,3,4}$ Integral breadths of the 1 0 0, 1 0 1, 1 0 2 and 1 1 0 lines, respectively (° 2θ).

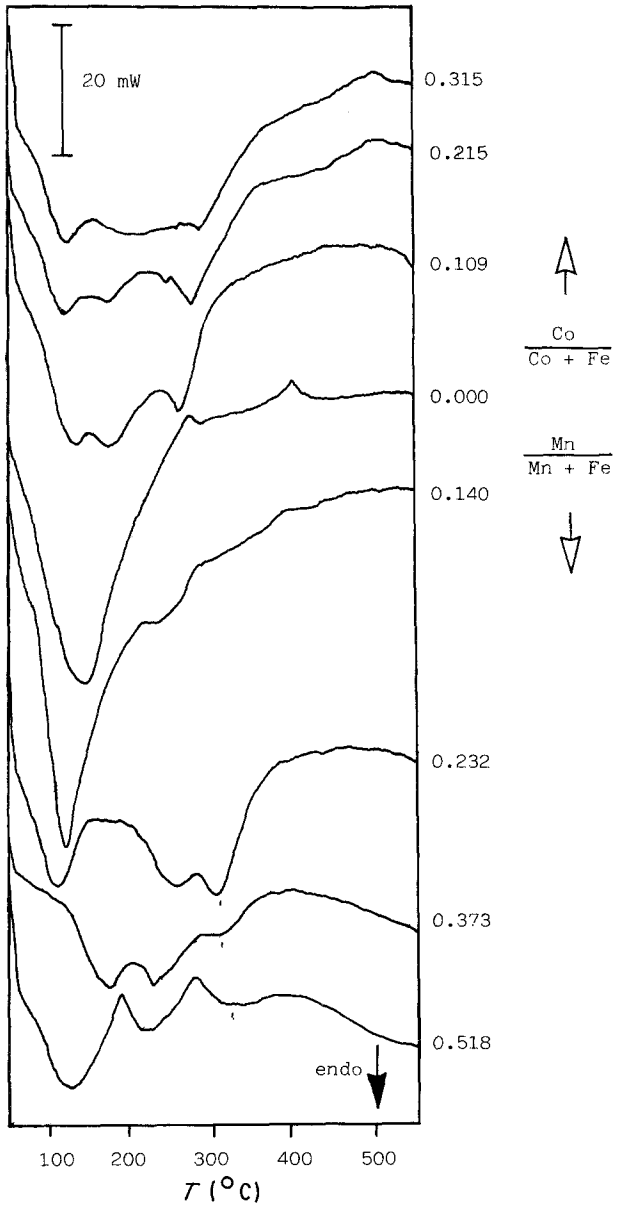

Figure 3 Differential scanning calorimetry traces of pure δ-FeOOH and manganese and cobalt containing samples.

On the other hand, the thermal behaviour of substituted δ-FeOOH was examined by DSC and TG data. The DSC traces in Fig. 3 recorded in static air atmosphere show that metal substitution leads to an increase in the decomposition temperature and a higher complexity of the endothermal effect. The multiple endotherm starts at about 100° C that can be assigned to the loss of surface water from the colloidal particles. For Co-containing samples the dehydroxilation endotherm is of multiple nature due to the presence of extra hydroxyles in the stoichiometry as a consequence of the Co(II) content. Additionally, in both manganese and cobalt substituted samples, several oxidation-reduction processes may take place. The TG traces of these samples showed a complex weight loss in the complete temperature interval, giving little information about the nature of the various processes.

In order to give new light on the thermal behaviour of the samples and to examine the nature of the oxides obtained from the thermal decomposition of the substituted oxyhydroxides, decomposed samples were prepared at 200, 400, 600 and 800° C by isothermal treatment during 1 h. At 200° C, the materials showed a highly distorted α-Fe_2O_3 structure characterized by an enhanced preferential line broadening of similar characteristics to that found in the product of decomposition of pure δ-FeOOH [9]. Due to the overlapping of these highly broadened profiles, a precise determination of lattice parameters could not be carried out. However, the determination of oxidation states led to values of 3 for cobalt and 4 for manganese, irrespective of the degree of substitution. It is noteworthy that an oxidation process seems to take place during this low temperature isothermal treatment leading to Mn(IV) and Co(III) ions exclusively. The weight gain corresponding to this oxidation process is undetected in the TG traces due to the simultaneous dehydroxilation weight-loss phenomena of higher magnitude. The presence of Mn(IV) in a distorted α-Fe_2O_3 structure could be explained in a similar way to the parent oxhyhydroxide by assuming cation vacancies. The similarity between the structures of both phases [15] and the high degree of distortion of the product phase may allow this possibility.

The samples prepared at 400° C were again single-phase products with α-Fe_2O_3 structure except for cobalt contents higher than 10% for which traces of a spinel phase were detected in the XRD patterns (Fig. 4). The oxidation states (Table II) showed the

TABLE II Stoichiometry and structural parameters of manganese and cobalt substituted α-Fe_2O_3 prepared by the thermal decomposition of δ-oxyhydroxide precursors at 400° C

Parameters	Mn, Fe						Fe	Co, Fe				
x^*	0.518	0.373	0.232	0.176	0.140	0.061	0.000	0.049	0.109	0.161	0.215	0.315
n†	3.428	3.129	3.000	3.000	3.000	3.000	–	2.959	2.890	2.814	2.647	2.600
a‡	0.4506	0.4960	0.5014	0.5023	0.5031	0.5039	0.5038	0.5027	0.5028	0.5019	0.4995	–
c‡	1.2880	1.3680	1.3730	1.3740	1.3790	1.3770	1.3710	1.3720	1.3720	1.3690	1.3610	–
β_1	3.233	1.895	1.534	1.590	1.802	1.903	1.444	1.540	1.752	2.673	1.888	–
D_1	7.800	17.900	18.300	14.800	15.000	10.900	26.500	10.300	11.800	7.200	7.500	–
$\tilde{e}_1$	34.600	20.700	15.000	14.600	18.200	17.200	14.200	10.100	15.300	24.300	11.800	–
β_2	1.351	1.030	0.884	0.932	0.961	1.074	0.932	0.930	0.865	1.240	1.065	–
D_2	167.000	254.000	791.00	521.000	326.000	163.000	436.000	625.000	360.000	145.000	127.000	–
$\tilde{e}_2$	10.200	7.000	7.500	7.700	6.600	4.500	7.800	8.010	5.000	7.400	0.100	–

x^* = M/(M + Fe); M = Co, Mn.
n† Oxidation state of M.
‡ Unit cell parameters (±0.002 nm).
$\beta_{1,2}$ Integral breadths of the 1 0 4 and 1 1 0 lines, respectively (deg 2θ).
$D_{1,2}$ Crystallite size (nm).
$\tilde{e}_{1,2}$ Microstrain content ($\times 10^3$).

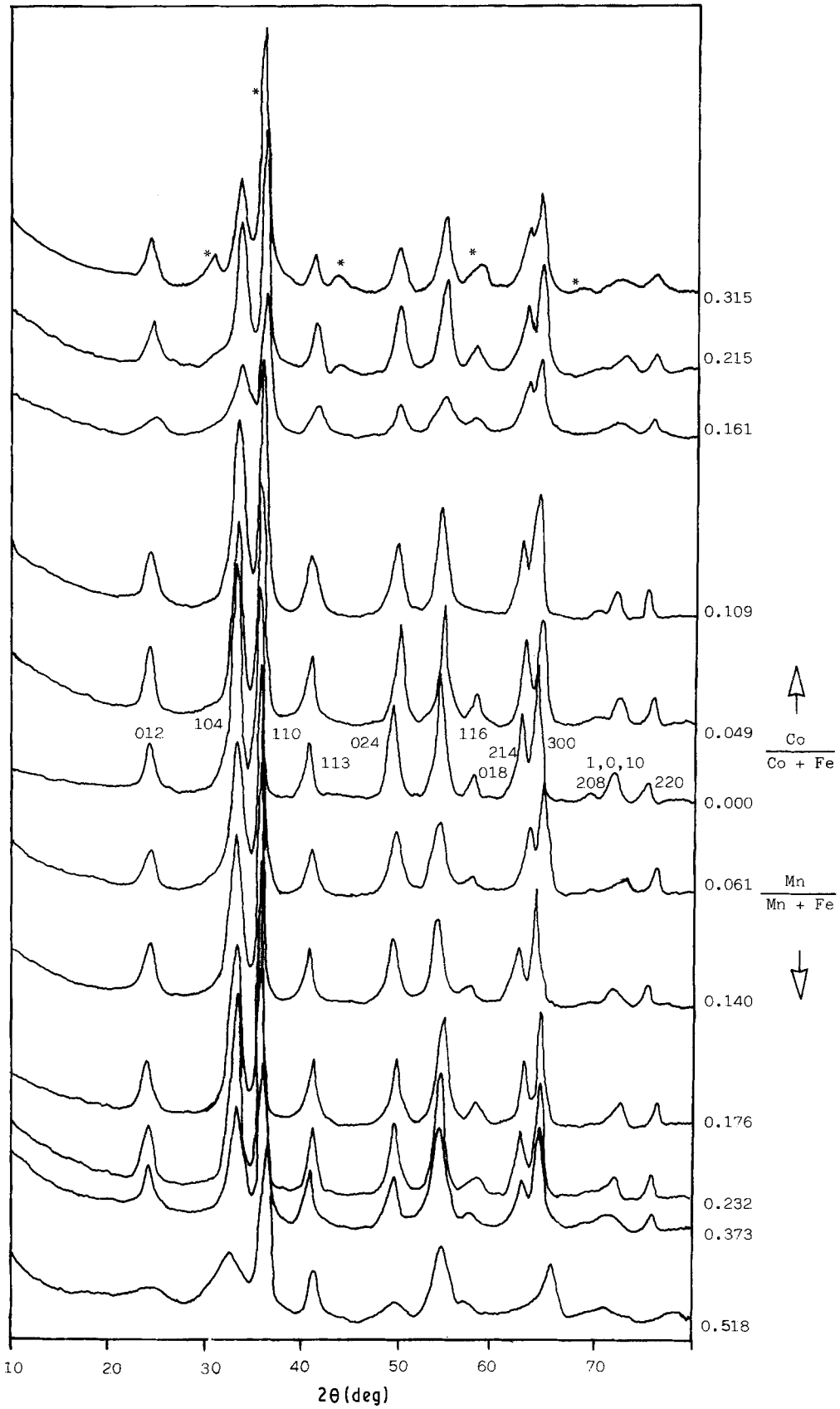

Figure 4 X-ray diffraction patterns of the decomposition products of the mixed oxyhydroxides at 400° C (*: spinel phases).

occurrence of a reduction process in the 200 to 400° C interval. This process was checked by recording DSC traces of the products prepared at 200° C (Fig. 5), where endothermal effects were observed at about 300° C. An analysis of the evolved gases during the thermal treatment, recorded under 10^{-3} dynamic vacuum revealed an H_2O release at about 260° C and a significant O_2 release between 310 and 370° C. These results indicate that the endothermic peak at this temperature in the complex DSC traces of Fig. 3 is due to reduction processes accompanied by a release of water that can be structurally bound as hydroxide in hematite-structure oxides. Similar behaviour has been reported in the literature for highly distorted "hydrohematite" [16] and in the thermal decomposition of divalent-metal substituted δ-FeOOH [8].

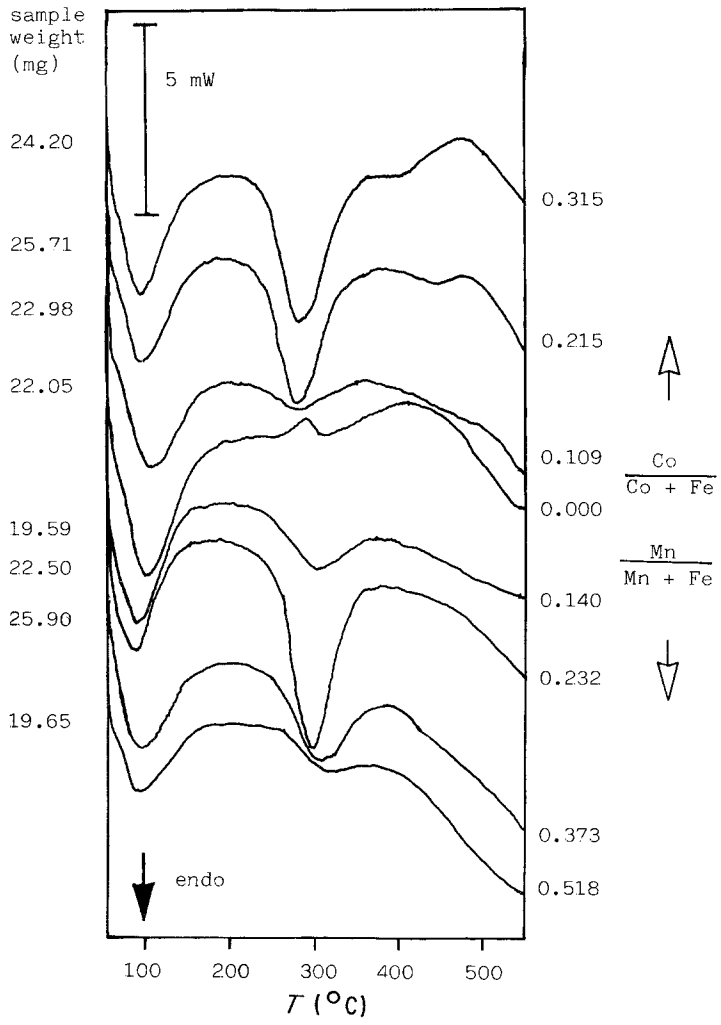

Figure 5 Differential scanning calorimetry traces of samples decomposed at 200° C.

Additionally, it should be noted that the oxidation states are now closer to those expected for stoichiometric sesquioxide for those Co-containing samples where no spinel oxide is detected and for manganese contents lower than 30%. As a consequence, crystallinity was improved considerably at this temperature. The unit cell parameters observed at 400° C (Table II) are in agreement with the ionic radii of the cations that are present. Thus, only those Mn-substituted samples where the presence of Mn(IV) was detected, show a sharp decrease in both a and c values. This fact is consistent with the absence of amorphous Mn(IV) oxides extruded from the substituted phase, as suggested in other systems [2].

Although crystallinity increases from 200 to 400° C, preferential line broadening is still observed. Line broadening analysis and electron microscopy were applied to study the imperfections present in these metastable solids. The results of XRD line broadening analysis for samples prepared at 400° C (Table II) show that the 1 0 4 lines are preferentially broadened by microstrain effects, in agreement with previous results on pure δ-FeOOH [9]. Additionally it is noteworthy that the size of the crystallites is also lower in the [1 0 4] direction, probably due to a platelike shape of the coherently diffracting domains.

On the other hand, the values of D and $\tilde{e}$ do not show a clear tendency with metal substitution. However, crystallite size in the [1 0 4] direction is always lower in substituted samples than in pure δ-FeOOH. This fact may be interpreted in terms of an easier separation of plates throughout the decomposition process for substituted samples, probably indicating an alternative distribution of cations in the original δ-oxyhydroxide structure. The bright field images (Fig. 2d, e) and dark-field electron micrographs obtained from the 1 1 0 Debye circles and diffraction spots (Fig. 2f, g) of the samples prepared at 200° C reveal that the particles are composed of few domains. This in agreement with the absence of a high broadening due to low crystallite size in $h\,k\,0$ diffraction lines observed for samples prepared at 400° C.

Finally, the thermal treatment of the samples at 600° C leads to mixtures of α-sesquioxide and spinel-related phases except for Mn-contents lower than 20%. At 800° C, traces of α-Mn_2O_3 are detected. Note should be taken of the higher stability of Mn-substituted α-Fe_2O_3 as compared with cobalt, due to the enhanced tendency of the latter to form mixed spinel phases with iron. This probably implies a higher homogeneity in composition for Mn-containing α-Fe_2O_{37} as described in previous studies on composition uniformity determined by relative solution procedures [17].

Acknowledgements

The authors acknowledge CICYT and FPI for financial support.

References

1. A. ROUSSET, F. CHASSAGNEUX and J. PARIS, *J. Mater. Sci.* **21** (1986) 3111.
2. A. FETLZ and M. JÄGER, *Reactiv. Solids* **6** (1988) 118.
3. J. M. JIMENEZ MATEOS, J. MORALES and J. L. TIRADO, *J. Solid State Chem.* **82** (1989) 87.
4. J. C. PETIT, *Compt. Rend.* **252** (1961) 3255.
5. S. OKAMOTO, *Kogyo Kagaku Zasshi* **67** (1964) 1845.
6. O. MULLER, R. WILSON and W. KRAKOW, *J. Mater. Sci.* **14** (1979) 2929.
7. W. KRAKOW, H. COLIJN and O. MULLER, *ibid.* **15** (1980) 119.
8. O. MULLER, R. WILSON, H. COLIJN and W. KRAKOW, *ibid.* **15** (1980) 959.
9. J. M. JIMENEZ MATEOS, J. MORALES and J. L. TIRADO, *J. Mater. Sci. Lett.* **5** (1986) 1295.
10. J. M. JIMENEZ MATEOS, J. MORALES and J. L. TIRADO, *J. Colloid Interface Sci.* **122** (1988) 507.
11. TH.H. DE KEIJSER, E. J. MITTEMEIJER and H. C. R. ROZENDAAL, *J. Appl. Cryst.* **16** (1983) 309.
12. M. PERNET, X. OBRADORS, J. FONTCUBERTA, J. C. JOUBERT and J. TEJADA, *IEEE Trans. Magn.* **MAG-20** (1984) 1524.
13. S. OKAMOTO, *J. Amer. Ceram. Soc.* **51** (1968) 549.
14. W. STIERS and U. SCHWERTMANN, *Geochim, Cosmochim, Acta* **49** (1985) 1909.
15. G. PATRAT, F. DE BERGEVIN, M. PERNET and J. C. JOUBERT, *Acta Crystallogr.* **B39** (1983) 165.
16. E. WOLSKA and W. SZAJDA, *J. Mater. Sci.* **20** (1985) 4407.
17. P. S. SIDHU, R. J. GILKES and A. M. POSNER, *Soil Sci. Soc. Am. J.* **44** (1980) 135.

Received 4 July
and accepted 12 December 1989